Clim Dyn
DOI 10.1007/s00382-011-1220-0

The simulation of medicanes in a high-resolution regional climate model

Leone Cavicchia · Hans von Storch

Received: 2 August 2011 / Accepted: 8 October 2011

Abstract Medicanes, strong mesoscale cyclones with tropical-like features, develop occasionally over the Mediterranean Sea. Due to the scarcity of observations over sea and the coarse resolution of the long-term reanalysis datasets, it is difficult to study systematically the multi-decadal statistics of sub-synoptic medicanes. Our goal is to assess the long-term variability and trends of medicanes, obtaining a long-term climatology through dynamical downscaling of the NCEP/NCAR reanalysis data. In this paper, we examine the robustness of this method and investigate the value added for the study of medicanes. To do so, we performed several climate mode simulations with a high resolution regional atmospheric model (CCLM) for a number of test cases described in the literature. We find that the medicanes are formed in the simulations, with deeper pressures and stronger winds than in the driving global NCEP reanalysis. The tracks are adequately reproduced. We conclude that our methodology is suitable for constructing multi-decadal statistics and scenarios of current and possible future medicane activities.

Keywords Mediterranean hurricanes · Dynamical downscaling · Mesoscale tropical-like cyclones · Medicanes climatology

L. Cavicchia (✉)
Centro Euro-Mediterraneo per i Cambiamenti Climatici, Bologna, Italy
e-mail: leone.cavicchia@cmcc.it

L. Cavicchia · H. von Storch
Institute of Coastal Research, Helmholtz-Zentrum Geesthacht, Geesthacht, Germany

L. Cavicchia
Ca' Foscari University, Venice, Italy

H. von Storch
Meteorological Institute, University of Hamburg, Hamburg, Germany

1 Introduction

1.1 Context of present study

Over the last decades, the occasional occurence over the Mediterranean Sea of sub-synoptic scale storms presenting several similarities with tropical cyclones has been reported. Given their resemblance to tropical storms, and in particular considering the strong winds associated with them, these systems have been referred to in the recent literature as "medicanes" (from *Medi*terrranean hurri*canes*).

Medicanes are considered rare phenomena, since only a few have been directly observed—the number of cases well documented in the literature is around ten. It has to be noted however that, due to their marine character and their sub-synoptic scale, most of the medicanes that have been observed and documented are the cases associated with impacts and damage on coastal areas. It is thus likely that a substantial number of medicanes that occurred in the past have not been detected at all.

Indeed, the availability of observations of such storms by in-situ weather reports is generally poor, and limited to ships cruising nearby. Since the 1980s, more cases have been detected by searching for structures similar to those of observed medicanes in satellite imagery (Tous and Romero 2011). However, due to the difficulty encountered in defining unequivocally a set of conditions to assess on firm

Published online: 29 October 2011

Table 1 Main features of the selected test cases

Event (YYMM)	Radius (km)	Lifetime (days)	Distance (km)	Eye	Genesis region
9501	150	3	~1,000	Yes	Ionian
0609	70	1	~500	No	Ionian
9609	150	1.5	~2,000	Yes	Balearic
9610	200	5	~3,000	Yes (twice)	Balearic

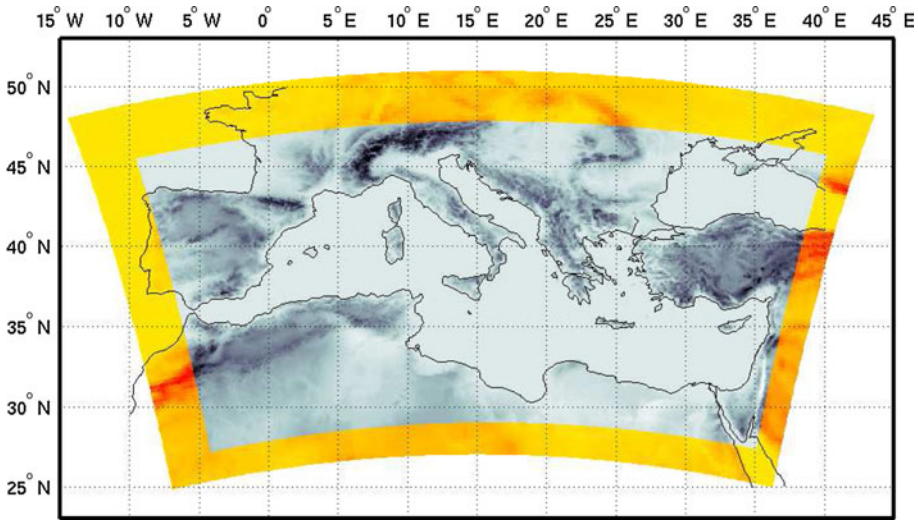

Fig. 1 Domains of the coarse (*yellow*) and high (*grey*) resolution simulations

grounds detection of medicanes, even after inspection of a large amount of satellite images the number of known medicanes is still limited to a few tens.[1]

Contemporary meteorological analyses capture most cases of medicanes because of high grid resolution and powerful initialisation techniques, which include the use of satellite data. However, when running frozen analysis systems, which are the basis of re-analysis such as NCEP/NCAR (Kalnay et al. 1996), a homogeneous description of the statistics of the sub-synoptic scale formation and life cycles of medicanes cannot be expected because of changing density and quality of observations on synoptic and sub-synoptic scales. Instead, changing statistics from such an inhomogeneous data set will represent more the effect of changing observational efficiency than changes in the physical phenomenon.

Thus, it is not possible to construct homogeneous statistics of the formation and life cycle of medicanes for the past decades by conventional data analysis or by analysing re-analyses. The same problem holds for the case of polar lows and for tropical cyclones. In both cases, a dynamical downscaling strategy has been employed, in which large-scale state descriptions provided by re-analysis are dynamically downscaled, using the concept of spectral nudging (von Storch et al. 2000), running an atmospheric limited area model in climate mode (Feser and von Storch 2008; Zahn et al. 2008). In the present study, we apply the same methodology to simulate the formation and life cycles of four medicanes studied in the literature (Reale and Atlas 2001; Davolio et al. 2009; Moscatello et al. 2008a, b; Homar et al. 2003; Lagouvardos et al. 1999; Pytharoulis et al. 2000). As in the previous studies on polar lows and typhoons, we examine how well known cases of the formation and life cycle of medicanes can be reproduced. We are not aware of any previous attempts to reproduce medicanes in climate mode simulations. Since our results are encouraging, we will in a second study run the system for the six decades of NCEP/NCAR reanalysis, to identify and track all medicanes and estimate their trends and variability.

The paper is organized as follows. In Sect. 2 we describe the experimental setup, the main features of the selected test cases and the model configuration. In Sect. 3 we discuss the model performance in reproducing the sea level pressure and wind patterns associated with medicanes, and how this information can be used to derive the storm track. In Sect. 4 we show how the model's ability to simulate the vertical structure of cyclones can be exploited to study the dynamical characterization of medicanes.

[1] A list of known medicanes cases is maintained on the website http://www.uib.es/depart/dfs/meteorologia/METEOROLOGIA/MEDICANES.

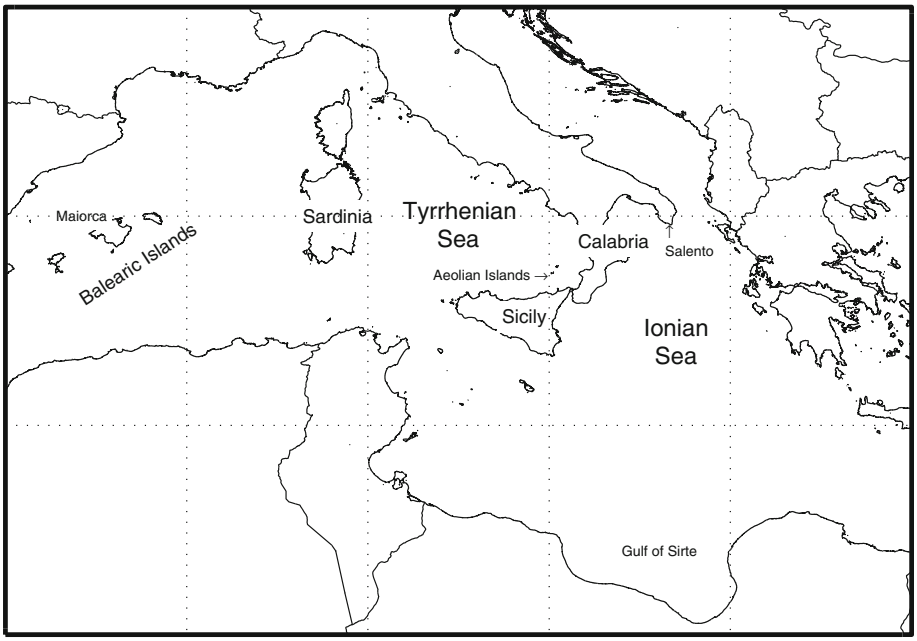

Fig. 2 Map of central Mediterranean including geographical locations mentioned in the text

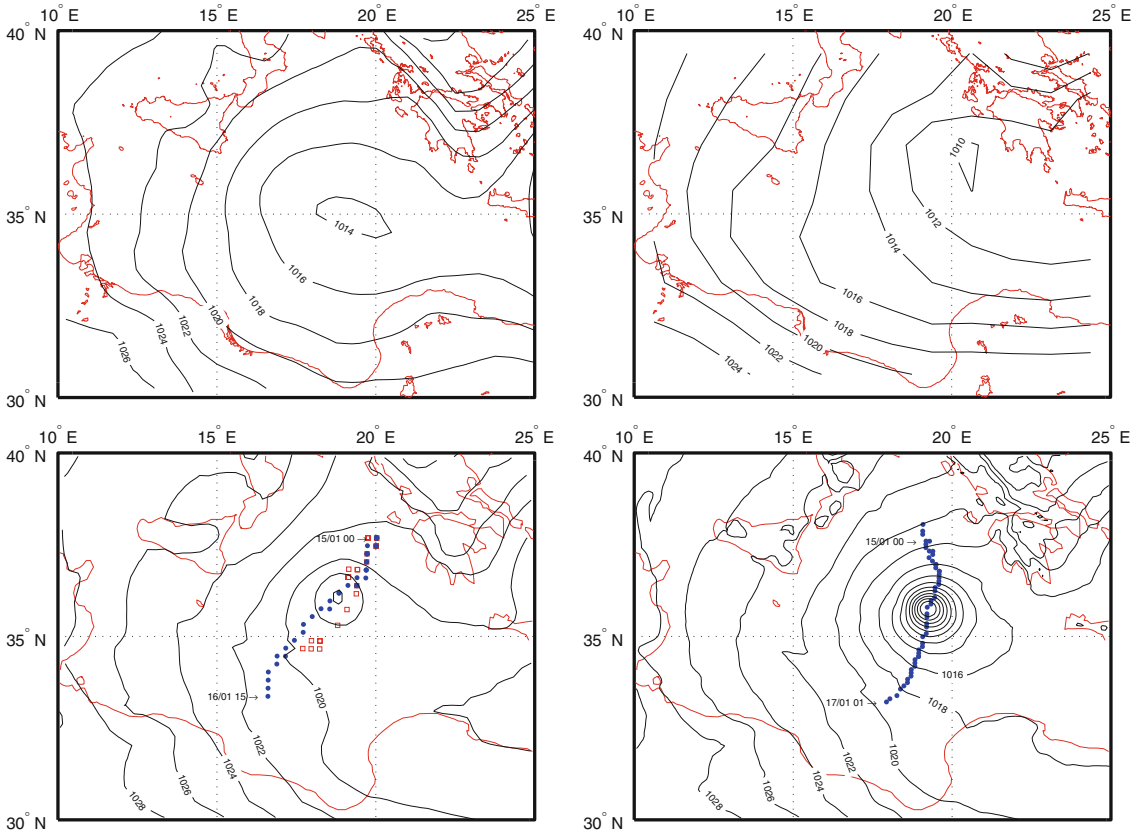

Fig. 3 Mean sea level pressure fields on January 16 at 00 UTC in the ECMWF analysis (*top left*), MERRA reanalysis (*top right*), and in the low resolution 9501sn2lo (*bottom left*) and high resolution 9501sn2hi (*bottom right*) simulations. Contour *lines* are plotted at 2 hPa intervals. The label 9501sn2lo/hi refers to the case of January 1995, and the 2nd simulation with a spectrally nudged formulation with low/high grid resolution. "dd/mm hh" labels indicate date and hour associated with the corresponding position. In the second panel *two different markers* have been used for a better visualization: *red empty squares* correspond to the part of the track where the storm was moving northwards, *blue filled circles* to the part where it was moving southwards

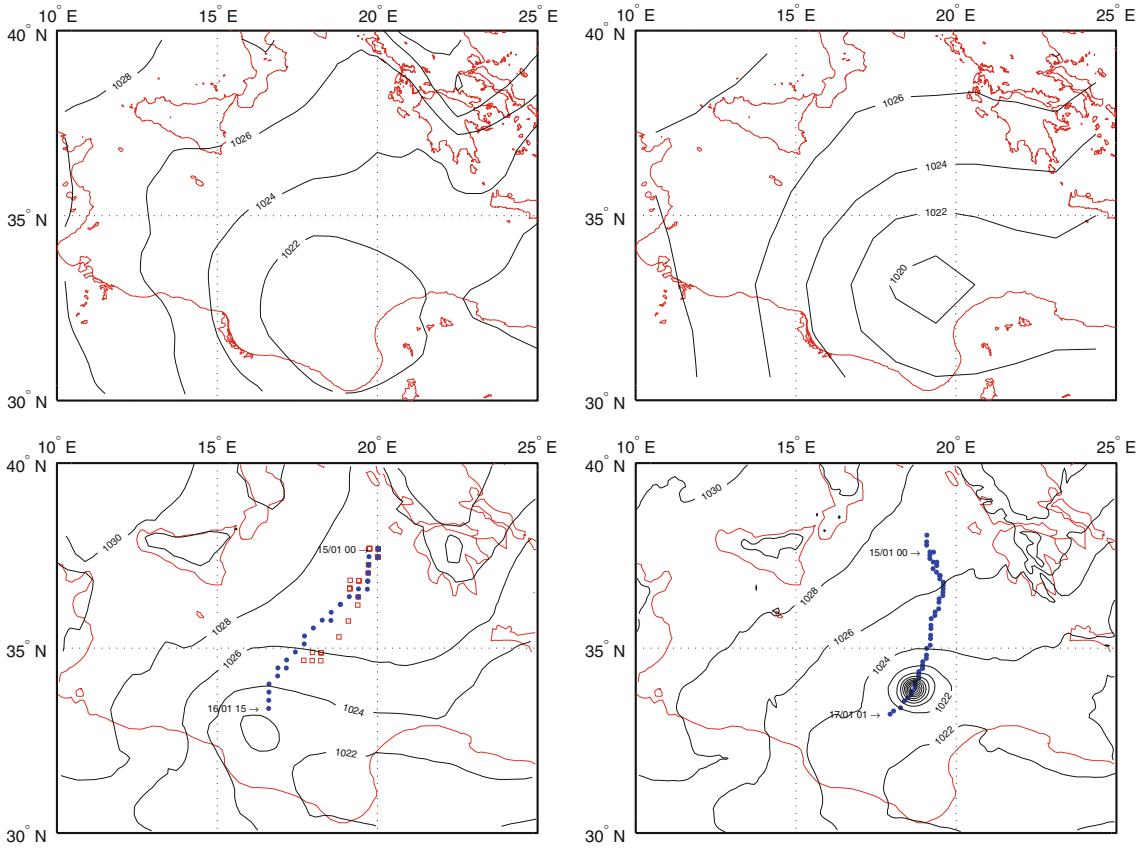

Fig. 4 The same of Fig. 3 on January 16 at 18 UTC

1.2 Medicanes

Medicanes resemble tropical cyclones (Emanuel 2005). They are indeed characterized—besides the associated winds that can reach hurricane speed—by a vertically symmetric structure, a cloud cover with a spiral shape and a cloud-free eye in the middle, and a warm core. Most of the cases occur during late summer and autumn.

The main features of medicanes and the typical values of their parameters, derived from the few observed events, can be summarized as follows:

- A *radius* between 70 and 200 km.
- A *lifetime* between ∼12 h and ∼5 days.
- The *travelled distance* is between ∼700 and ∼3,000 km.
- A clearly defined *eye* develops in most cases, and is visible for as long as 3 days. In some cases the eye does not appear, while in some others it develops twice (disappearing when the storm crosses land areas).
- *Wind speed* up to ∼40 m/s.
- The most frequent *genesis regions* are the Balearic islands and the Ionian sea.
- Most of the medicanes occur during *autumn*, but some have been detected also in winter and spring.

The formation of sub-synoptic scale storms with tropical-like features over relatively cool waters, in comparison with the empirical threshold of 26°C derived from the analysis of tropical cyclones, is not an isolated phenomenon; similar storms, the polar lows, have long been known to develop over high latitude oceans (Rasmussen and Turner 2003).

It has been shown, from a theoretical perspective, how the presence of a cold low in the upper layers of the atmosphere over warm enough waters can provide an environment favourable to the formation of medicanes (Emanuel 2005). Numerical process studies confirmed the role played by this mechanism in the development of some of the observed medicanes (Fita et al. 2007).

2 Experimental setup

2.1 Test cases

We selected four different test cases of historical medicanes documented in the literature to be reproduced in the model simulations. The main characteristics of these cases are reported in Table 1.

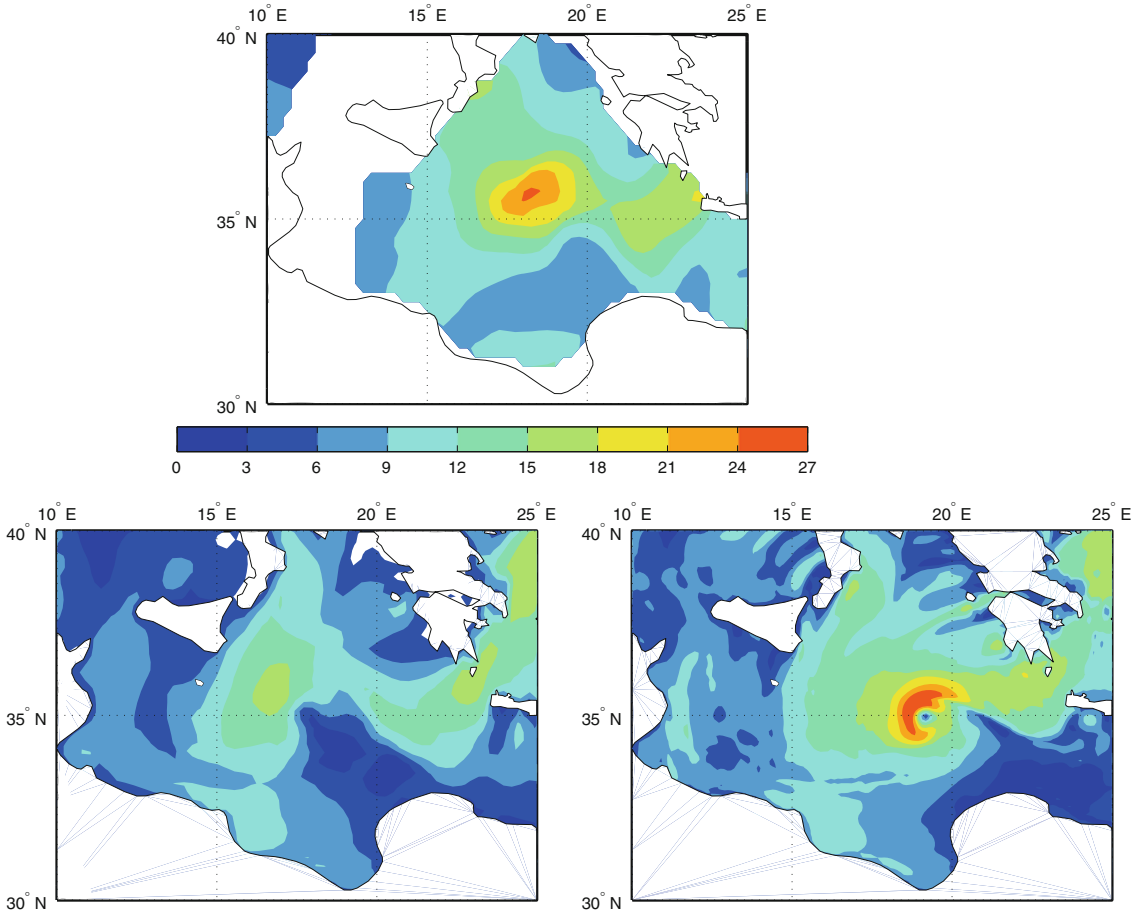

Fig. 5 Measured wind speed field on January 16 at 18 UTC as reconstructed in the NOAA "Blended Sea Winds" (*top*). 10-m wind speed in 9501sn2lo (*bottom left*) and 9501sn1hi (*bottom right*) simulations. Every contour represents a 3 m/s increment. The label 9501sn2lo/hi refers to the case of January 1995, and the 2nd simulation with a spectrally nudged formulation with low/high grid resolution

The choice of these particular events is motivated by the fact that they span a wide range of the typical phenomenological parameters of medicanes, including both typical and extreme values. They are all from recent decades, when observational coverage by satellites was good, and when operational analyses, as done by ECMWF, have good skills also on sub-synoptic scales (Simmons 2006), so that we have adequate data available for assessing the quality of our simulations. Indeed, we use the following observational data for validation:

1. the NOAA "SeaWinds" product at 6-h time resolution (Zhang et al. 2006). SeaWinds contains gridded, high resolution ocean surface vector winds and wind stresses on a global 0.25° grid for the period 9 July 1987—present. The wind speeds are generated by blending observations from instruments mounted on multiple satellites. The accuracy of scatterometer-based wind retrievals is very good for winds up to 20 m/s, while it is highly diminished for stronger winds (see e.g. Ebuchi et al. 2002; Ricciardulli and Wentz 2011)
2. Mean sea level pressure fields from ECMWF operational analysis data, at 0.25° grid resolution.

In order to assess the added value of the dynamical downscaling approach, we also compare the model results with a state-of-the-art reanalysis product, the NASA's MERRA reanalyses (Rienecker et al. 2011), featuring a 0.5° horizontal resolution and 72 vertical levels.

2.2 Dynamical downscaling approach

The downscaling is performed in the CCLM atmospheric limited area model (Rockel et al. 2008), the climate version of the COSMO weather model. The model features non-hydrostatic equations and has 32 σ vertical levels.

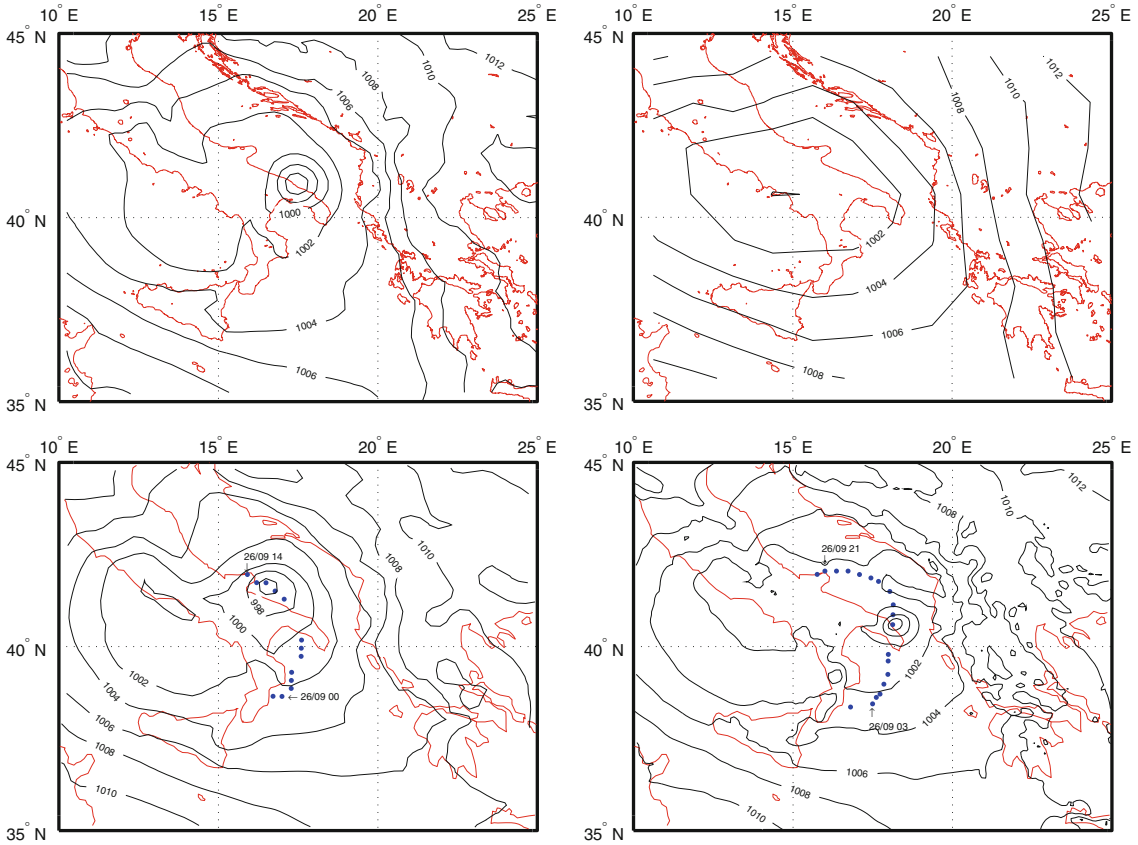

Fig. 6 Mean sea level pressure fields on September 26 at 12 UTC in the ECMWF analysis (*top left*), MERRA reanalysis (*top right*), 0609sn2lo (*bottom left*) and 0609sn2hi (*bottom right*) simulations. *Contour lines* are plotted at 2 hPa intervals. The label 0609sn2lo/hi refers to the case of September 2006, and the 2nd simulation with a spectrally nudged formulation with low/high grid resolution. "dd/mm hh" *labels* indicate date and hour associated with the corresponding position

We employ two different horizontal resolutions. The "low" resolution simulations use a 0.22° (∼25 km) grid on a domain of 176 × 106 grid points (see Fig. 1) and are driven by initial and boundary conditions derived from NCEP/NCAR reanalyses (Kalnay et al. 1996). The domain covers the whole Mediterranean Sea and the main mountain ranges around it. The grid spacing of 0.22° is the finest that can be used for a single nested downscaling of NCEP/NCAR reanalyses, since the model performance decreases for downscaling factors higher than 10. We use the NCEP/NCAR reanalyses, which will be employed in the long integrations, because of their longer period of coverage. Although higher resolution reanalysis products are available, these cover shorter time periods.

The "high" resolution simulations are run at 0.09° (∼10 km) in a double nested configuration, on a domain of 386 × 206 grid points (see Fig. 1). Other than the grid resolution, the two model versions do not differ.

For each of the test cases under study, two ensembles of four simulations each are produced. The ensemble members differ in their start dates, which are separated by intervals of 24 h. In order to ensure that the simulation results do not depend on initial conditions ("climate mode"), the starting date preceeds the formation of the medicane by about 2 weeks.

In the first ensemble the evolution of atmospheric variables is forced only through initial and lateral boundary conditions. The members of this ensemble are labelled as "YYMMnn1lo/hi"–"YYMMnn4lo/hi". In the second ensemble there is an additional forcing in the interior of the domain, derived from spectrally nudging wind above 850 hPa. The simulations of this ensemble will be referred to as "YYMMsn1lo/hi"–"YYMMsn4lo/hi".

The aim of spectral nudging (von Storch et al. 2000) is to force the large scale components of the atmospheric fields to stay close to the reanalyses, while the small scale components are left free to evolve in the regional model. Spectral nudging is applied on the wind field components, for scales larger than 4 NCEP/NCAR grid points, corresponding to 1,000 km. Moreover, nudging is applied only on vertical levels above 850 hPa, while wind in the lower layers is left free to interact with the local orography. In

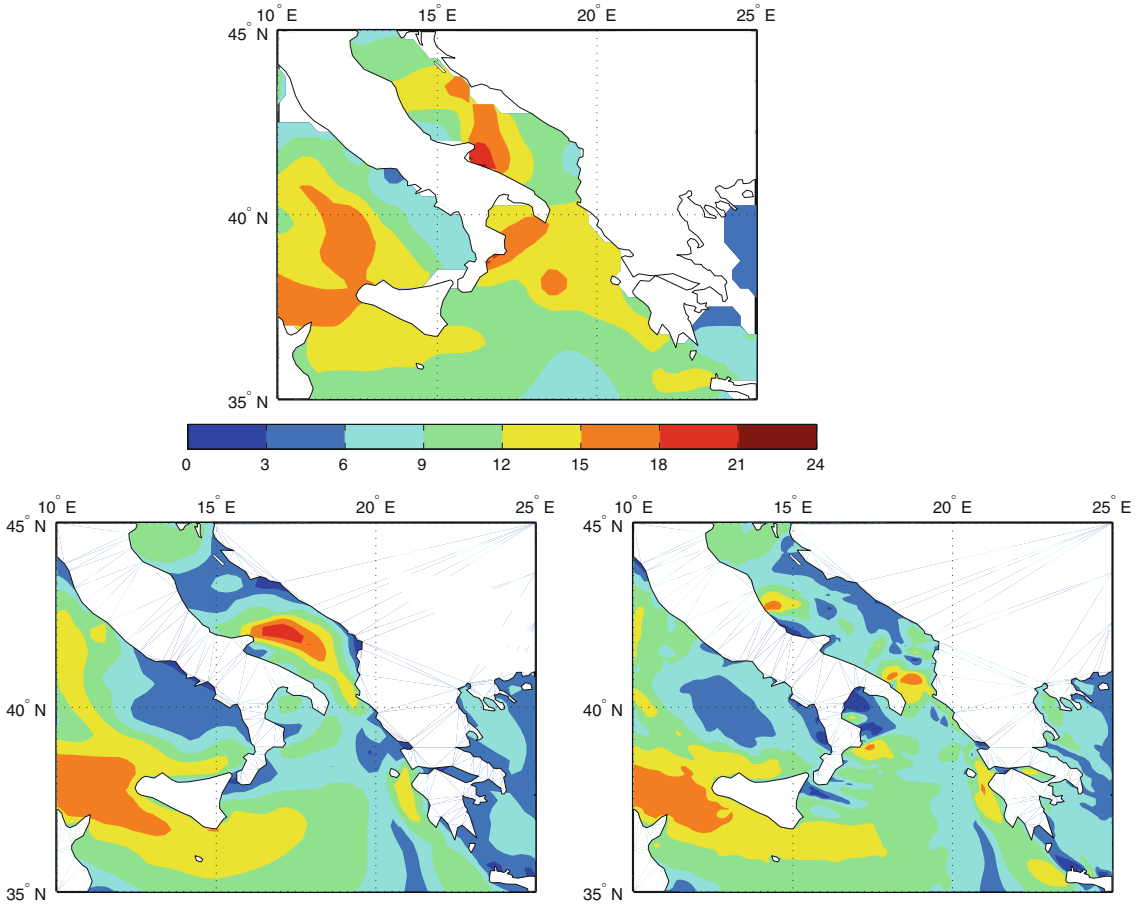

Fig. 7 Measured wind speed field on September 26 at 12 UTC as reconstructed in the NOAA "Blended Sea Winds" (*top*). 10-m wind speed in 0609sn2lo (*bottom left*) and 0609sn2hi (*bottom right*) simulations. Every contour represents a 3 m/s increment. The label 0609sn2lo/hi refers to the case of September 2006, and the 2nd simulation with a spectrally nudged formulation with low/high grid resolution

both the low and high resolution simulations the values of the atmospheric fields used as a reference in spectral nudging are the ones provided by the NCEP/NCAR reanalysis.

2.3 Tracking

A simple tracking procedure is applied, consisting of two steps. First, pressure minima are searched for and recorded in the hourly model outputs; then a clustering algorithm assigning to the same track the pressure minima within a radius of 100 km at two consecutive timesteps is applied.[2]

The following conditions (most of which are adapted from Zahn et al. (2008); Zahn and von Storch (2008)) are enforced:

- Only pressure minima associated with a pressure gradient greater than 25 Pa over two gridpoints are recorded (this choice makes the threshold resolution-dependent, coherently with the increase in the depth of simulated cyclones with model resolution).
- Only pressure minima detected in a grid box with a land fraction smaller than 40% are recorded.
- Tracks composed of less than five points (corresponding to a duration shorter than 5 h) are discarded.
- In order to avoid spurious signals along the coast, only tracks with at least three points in a grid box with strictly no land content are considered.
- Tracks with a distance between the starting and final points smaller than 100 km are not taken into account, in order to discard persistent stationary lows.

3 Results: surface patterns

In this section we discuss the model's ability in reproducing the sea level wind and pressure patterns associated with the medicane test cases under study. We begin by

[2] In a few cases where there are gaps in the reconstructed track, for example due to the cyclone crossing an island, the single parts have been assigned to the same track manually.

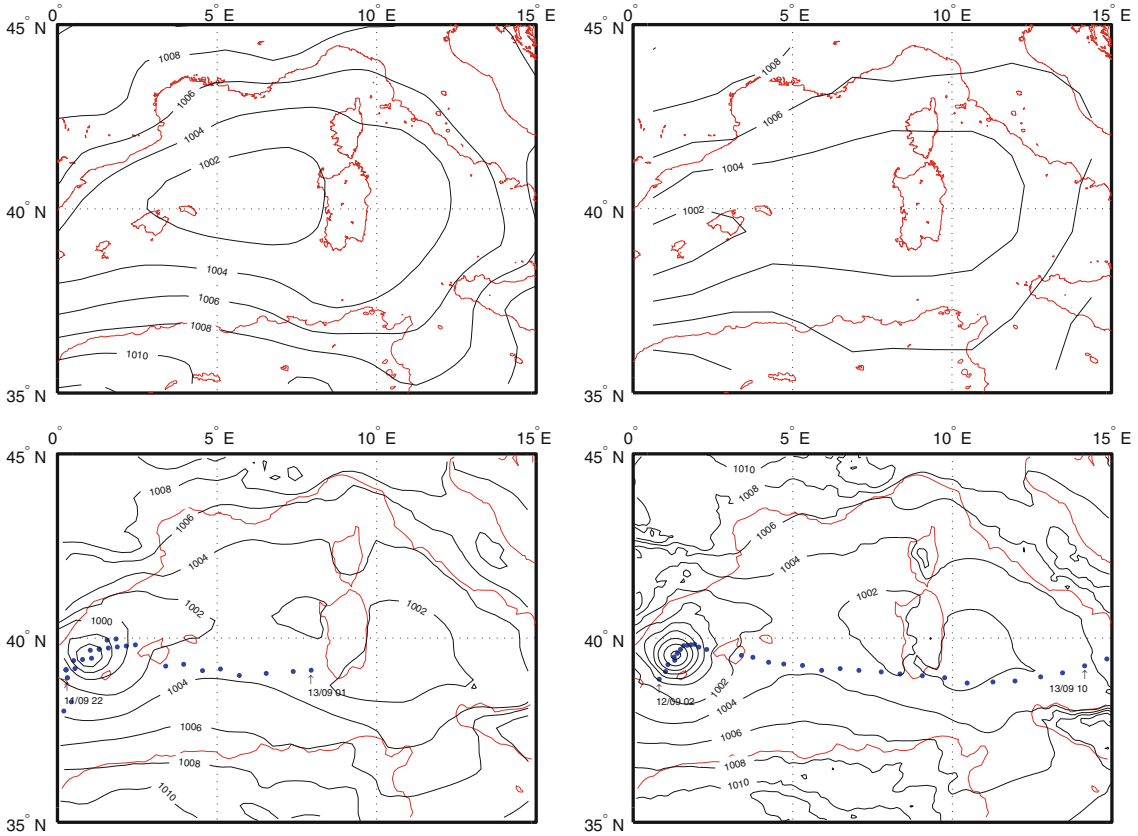

Fig. 8 Mean sea level pressure fields on September 12 at 06 UTC in the ECMWF analysis (*top left*), MERRA reanalysis (*top right*), 9609sn2lo (*bottom left*) and 9609sn2hi (*bottom right*) simulations. *Contour lines* are plotted at 2 hPa intervals. The label 9609sn2lo/hi refers to the case of September 1996, and the 2nd simulation with a spectrally nudged formulation with low/high grid resolution. "dd/mm hh" *labels* indicate date and hour associated with the corresponding position

discussing only the 2nd realization of the spectrally nudged simulations, i.e, YYMMsn2lo and YYMMsn2hi, in low and high resolution. The rationale for doing so will become clear in Sect. 3.5, when we demonstrate that the spectrally nudged simulations are very close to each other, while the non-nudged cases show some divergence.

3.1 15 January 1995 medicane

The January 1995 case (Lagouvardos et al. 1999; Pytharoulis et al. 2000) is probably the most well known medicane, due to the striking similarities between its cloud pattern visible in satellite imagery and those of tropical cyclones.

Synoptic analysis show a larger scale low moving from the central Mediterranean (Fig. 2), northwards of Libya, towards the Ionian coast of Greece in the two days preceding the medicane formation. Ships crossing the Ionian sea measured winds up to 30 m/s associated with the precursor low. By the night of January 15, as the disturbance had reached the coast of Greece, satellite pictures reveal a structure presenting typical hurricane features, that originated in the center of the large scale low and remained approximately stationary as the parent low kept moving eastwards towards the Aegean Sea and Turkey. During the following afternoon the medicane started to move southwestwards and kept travelling towards the coast of Lybia during the following 48 h; during that time observations by ships cruising the Mediterranean reported strong winds, heavy precipitation and positive temperature anomalies in the vicinity of the center of the storm. After making landfall in the Gulf of Sirte the storm dissipated in the next few hours.

Figure 3 shows a comparison of mean sea level pressure on January 16 at 00 UTC in ECMWF analysis, MERRA reanalysis, and in 25 km resolution and 10 km resolution simulations, together with the medicane track as reconstructed, respectively, in the low resolution and high resolution simulations. In both cases, with the pressure thresholds used, the storm disappears before reaching the Lybian coast. In the low resolution simulation, the part of the track where the storm was moving northwards (marked

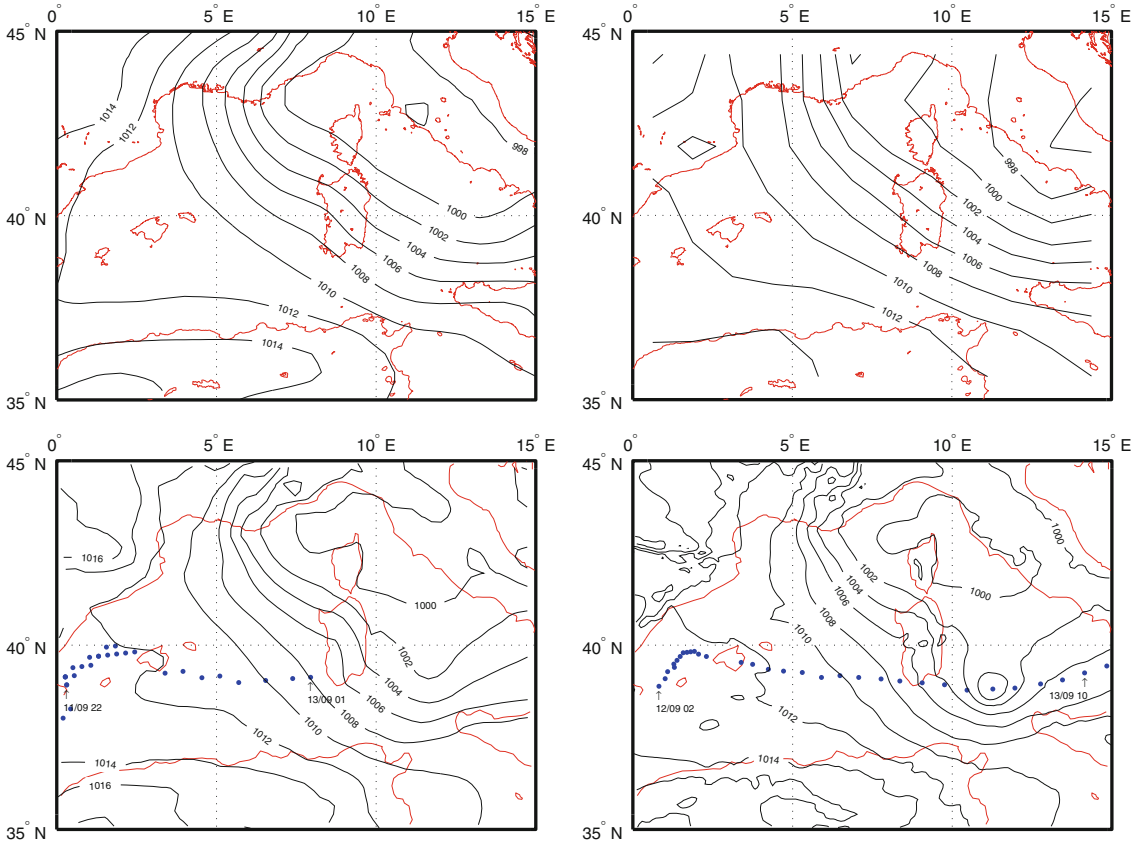

Fig. 9 The same of Fig. 8 on September 13 at 06 UTC

with red squares) corresponds roughly to the development of the medicane in the core of the precursor low; the second part (blue dots) corresponds to the life cycle of the fully developed medicane, after it had split from the parent low. In the high resolution simulation the first part of the track does not appear because the corresponding pressure minima are less deep and less steep. There is a good agreement on the position of the pressure minimum in the four charts. The pressure value at the minimum is 1,014 hPa in the ECMWF diagram, 1,010 hPa in the MERRA reanalysis, 1,016 in the coarse resolution, and 1,000 hPa in the high resolution run.

Figure 4 shows the same fields of Fig. 3 18 h later, on January 16 at 18 UTC. The difference in the positions of the central pressure minima in the two simulations has increased to a few hundred kilometers. The minimum pressure value is 1,022 hPa in the ECMWF analysis, 1,020 hPa in the MERRA reanalysis, 1,022 hPa in the coarse resolution simulation, and 1,006 hPa in the high resolution simulation.

Figure 5 shows a snapshot of the wind speed in NOAA measurement and model simulations on January 16 at 06 UTC. In the satellite measurement the observed wind speed reaches a maximum value of approximately 25 m/s. In the low resolution simulation this value is underestimated by about 30%. In the high resolution simulation, on the other hand, the maximum wind speed agrees with the measured value; moreover, the fine structure of the wind pattern is visible, showing a windless air column above the pressure minimum, corresponding to the cyclone's eye.

3.2 26 September 2006 medicane

The September 2006 medicane (Davolio et al. 2009; Moscatello et al. 2008a, b; Miglietta et al. 2011; Conte et al. 2011) has the smallest radius and shortest lifetime among all known cases. Moreover, it is the only case among the four considered in this work where a well defined eye does not develop at any stage of the storm evolution. It is therefore expected to be a representative test for the model ability to reproduce smaller medicanes.

The synoptic and observational analysis (Moscatello et al. 2008b) shows a cyclonic disturbance moving across the Strait of Sicily and travelling northwards over the Ionian Sea along the coast of Calabria on September 25th.

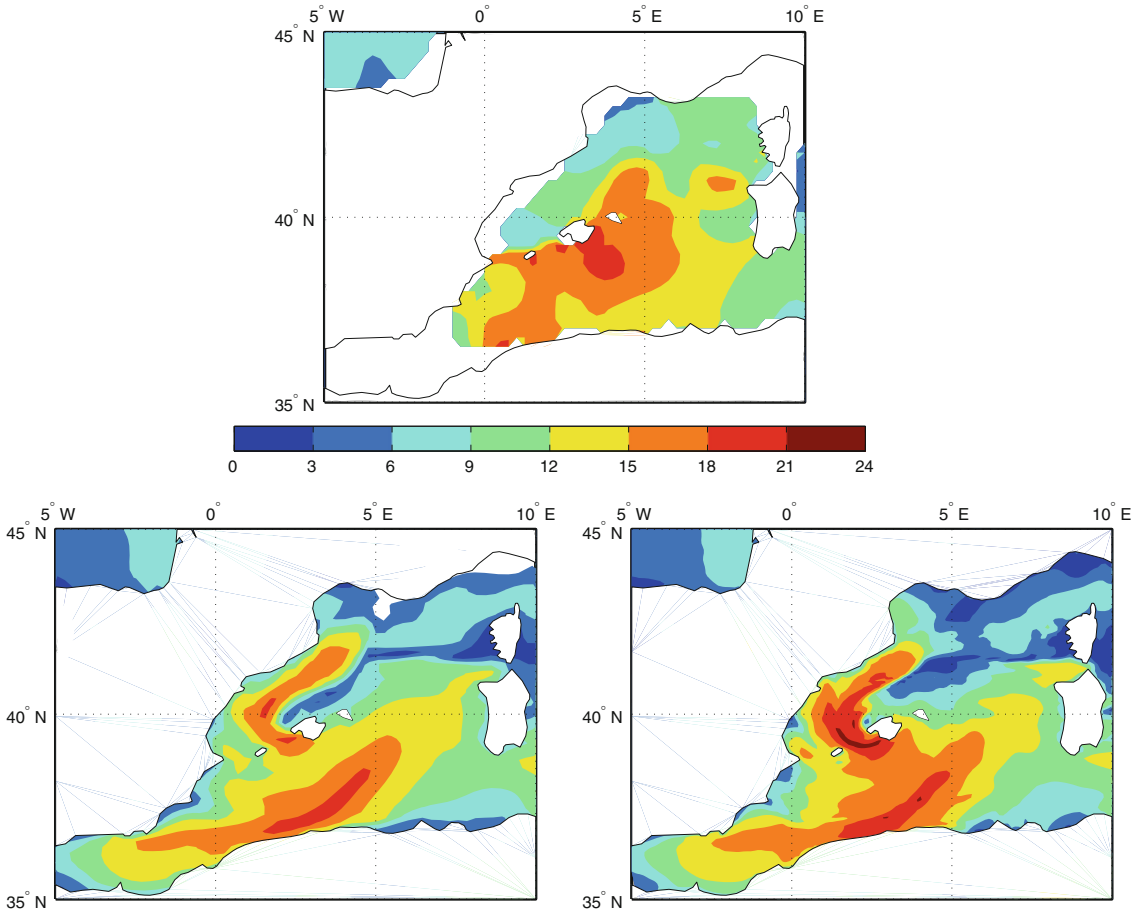

Fig. 10 Measured wind speed field on September 12 at 12 UTC as reconstructed in the NOAA "Blended Sea Winds" (*top*). 10-m wind speed in 9609sn2lo (*bottom left*) and 9609sn2hi (*bottom right*) simulations. Every contour represents a 3 m/s increment. The label 9609sn2lo/hi refers to the case of September 1996, and the 2nd simulation with a spectrally nudged formulation with low/high grid resolution

The numerical analysis in Moscatello et al. (2008a) shows that the cyclone was formed the previous night in the lee of the Atlas mountains. During the night of September 26 a strong deepening is observed and, as the cyclone reached the western coast of Salento the following morning, it had evolved to a medicane. The storm then crossed the Salento peninsula, where extreme wind speeds were measured by ground stations and several damages were produced. It finally traveled northwestwards over the Adriatic Sea and the afternoon of the same day it made landfall on northern Apulia, where it rapidly dissipated.

Mean sea level pressure on September 26 at 12 UTC in ECMWF operational analysis, MERRA reanalysis, and model simulations, along with the medicane track as reconstructed in the low resolution and high resolution simulations, is shown in Fig. 6. The displacement in the minimum position between the two model simulations reflects the different storm velocities. The pressure value at the minimum is 996 hPa in the ECMWF analysis, coarse resolution simulation, and high resolution simulation. The medicane is not visible in the MERRA reanalysis.

Wind speed in satellite observation and model simulations on September 26 at 12 UTC is shown in Fig. 7. The maximum wind speed of 22 m/s reported in the satellite measurements is reproduced with good accuracy in the low resolution simulation, while it is underestimated by about 10–15% in the high resolution simulation. It has to be noticed however that, due to the different storm propagation speeds in the two simulations, the fixed-time snapshots might not represent the same phase of the evolution of the actual storm.

3.3 12 September 1996 medicane

The case of September 1996 (Homar et al. 2003) is an example of a typical medicane developing in the Balearic region, one of the areas where medicanes formation is more often encountered.

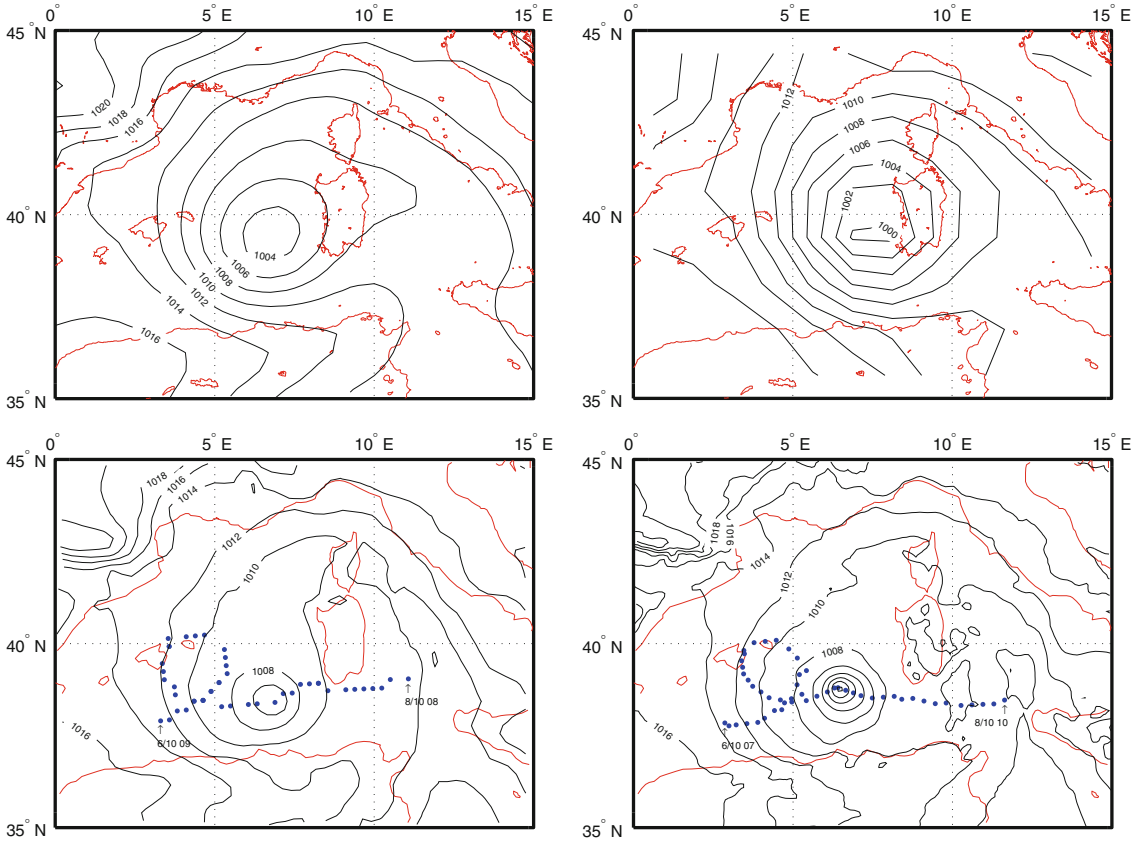

Fig. 11 Mean sea level pressure fields on October 7 at 18 UTC in the ECMWF analysis (*top left*), MERRA reanalysis (*top right*), 9610sn2lo (*bottom left*) and 9610sn2hi (*bottom right*) simulations. *Contour lines* are plotted at 2 hPa intervals. The label 9610sn2lo/hi refers to the case of October 1996, and the 2nd simulation with a spectrally nudged formulation with low/high grid resolution. "dd/mm hh" *labels* indicate date and hour associated with the corresponding position

The system developed between the night and early morning of September 12 off the Valencian coast, where heavy rainfall was reported; an eye structure was already fully developed at the end of this first stage. During the morning of September 12 the storm started to move quickly eastwards crossing Maiorca and later in the day the southern extremity of Sardinia. During the following night, the medicane made landfall on the coast of southern Italy and it dissipated.

Figure 8 shows mean sea level pressure charts on September 12 at 06 UTC from ECMWF analysis, MERRA reanalysis, and model simulations, and the medicane track as reconstructed in the 25 and 10 km resolution simulations. While the track in the coarse resolution simulation ends as the storm reaches Sardinia, in the high resolution simulation the storm is tracked until it reaches the Italian coast. The mesoscale low structure corresponding to the medicane is not visible in the ECMWF and MERRA pressure fields. However analysis of satellite pictures confirms the presence of the storm (see Figs. 1a and 2a in Luque et al. 2007). The value of the pressure minimum is 996 hPa in the coarse resolution, and 990 hPa in the high resolution run.

Figure 9 shows the pressure distributions 24 h later, after the storm has crossed southern Sardinia. At this stage of the storm evolution, closed isobars are not visible either in the ECMWF and MERRA pressure charts or in the coarse resolution simulation. The medicane is still clearly visible in the high resolution simulation, with a pressure minimum of 1,000 hPa.

Figure 10 shows the wind speed in NOAA observations and model simulations on September 12 at 12 UTC. Both the satellite measurement and the coarse resolution simulation show a maximum wind value of about 20 m/s, while in the high resolution simulation this value reaches 24 m/s. The characteristic pattern associated with the storm eye is clearly visible in the high resolution simulation.

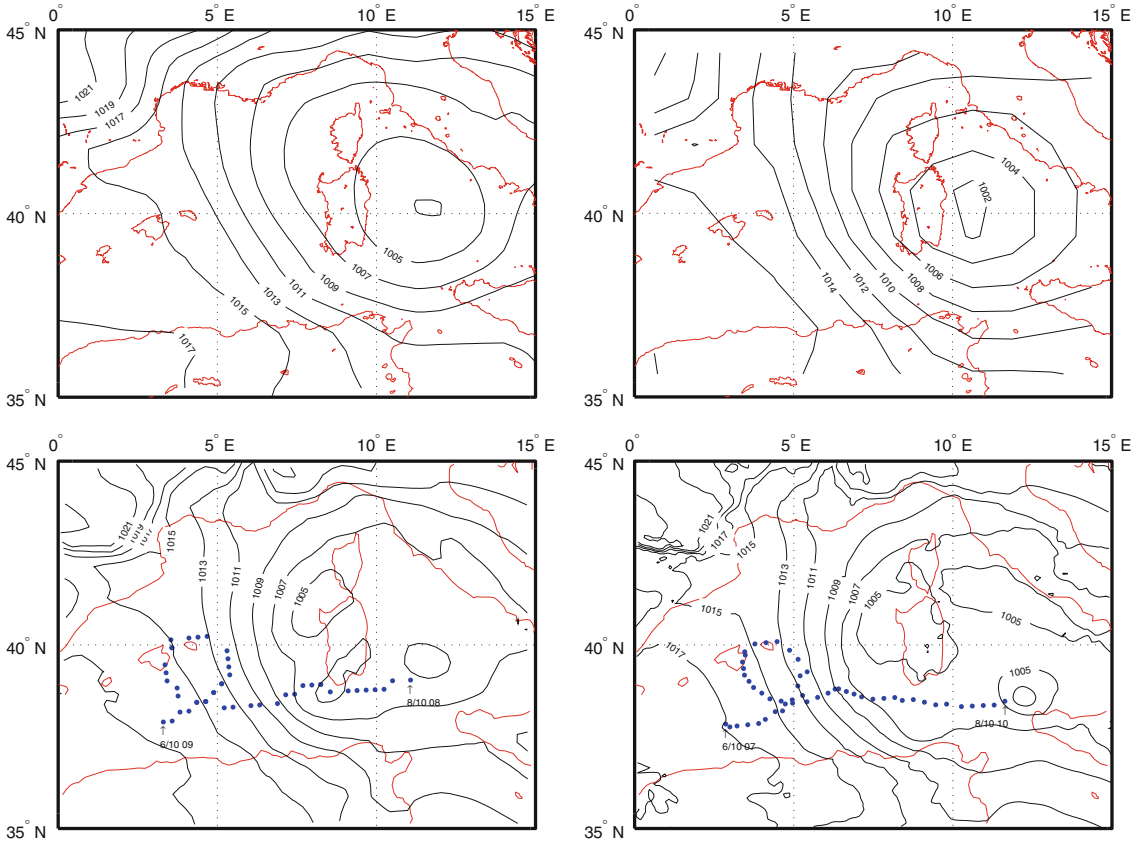

Fig. 12 The same of Fig. 11 on October 8 at 12 UTC

3.4 7 October 1996 medicane

The 6 October 1996 case (Reale and Atlas 2001) has one of the longest lifetime and largest radius among the known medicanes. During October 6th the medicane developed northwards of Algeria and deepened while it was moving between the Balearic islands and Sardinia. There are no surface observations available for this part of the track, but satellite pictures show a well defined eye-like structure. On the night of October 8 while the storm was crossing southern Sardinia, it weakened and the eye structure was lost. In the following morning however, as the cyclone traveled eastwards over the Tyrrenian Sea, it deepened and a smaller eye developed again. Several surface reports about 100 km off the center of the storm indicate winds of 25 m/s. On October 9, as the medicane was travelling north of Sicily, severe damages caused by extreme winds were reported in the Aeolian islands. The medicane started to dissipate while moving southeastwards across Calabria.

Figure 11 shows the mean sea level pressure distribution on October 7 at 18 UTC in ECMWF analysis, MERRA reanalysis, and in the coarse and high resolution simulations, and the medicane track as reconstructed in model simulations. With the thresholds used the storm is tracked only until it approaches the western part of Sicily. There is a good agreement on the position of the pressure minimum in the different charts. The minimum pressure value is 1,004 hPa in the operational analysis, 1,000 hPa in the MERRA reanalysis, 1006 hPa in the 25 km resolution simulation, and 998 hPa in the 10 km resolution simulation.

Figure 12 shows the pressure distributions 18 h later, after the storm has crossed Sardinia. The difference in the positions of the central pressure minima has grown to a few hundred kilometers. The minimum pressure value is 1,003 hPa in the ECMWF analysis, 1,002 hPa in the MERRA reanalysis, 1,005 hPa in the low resolution simulation, and 1003 hPa in the high resolution simulation.

Figure 13 shows the wind speed in satellite measurement and model simulations on October 7 at 18 UTC. There is an evident mismatch between observations and simulations in the wind speed values of the background pattern. This is probably due to the presence of a Mistral outburst, corresponding to the darker area in the upper part

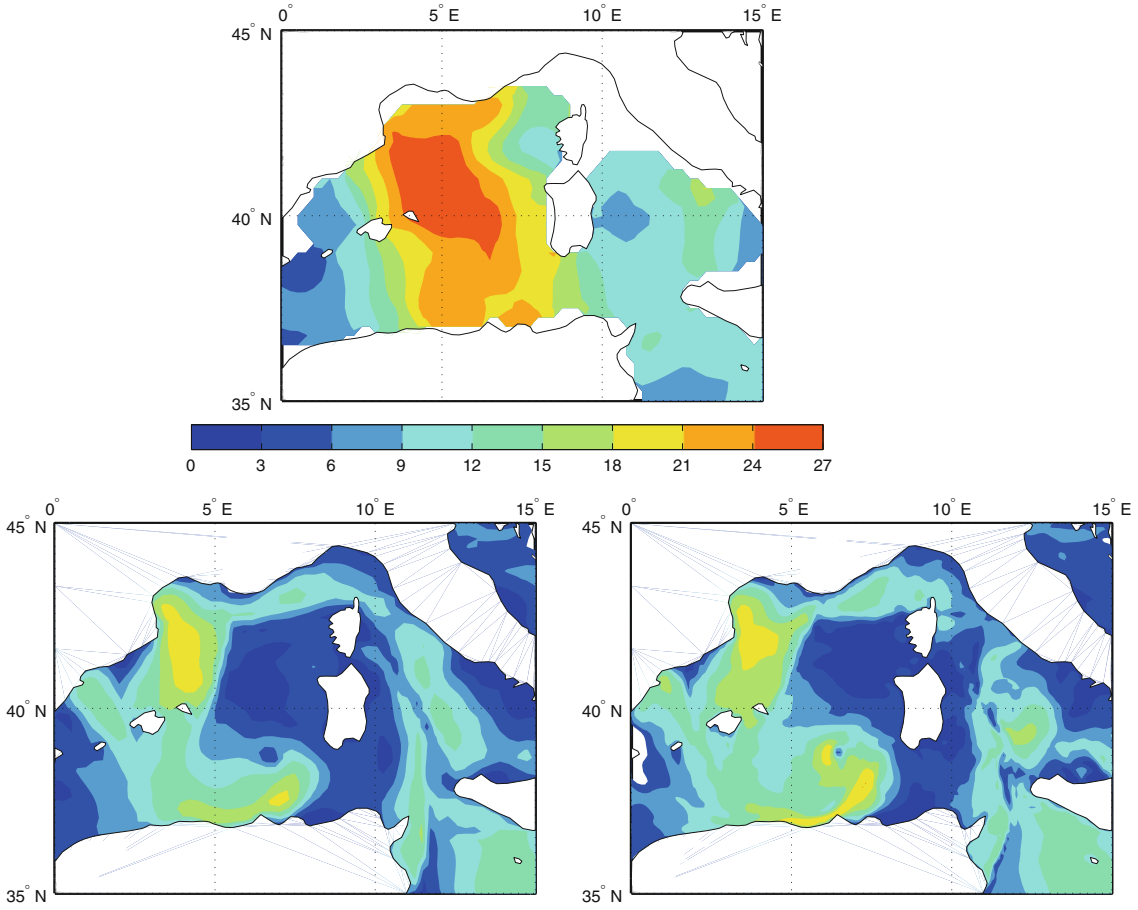

Fig. 13 Measured wind speed field on October 7 at 18 UTC as reconstructed in the NOAA "Blended Sea Winds" (*top*). 10-m wind speed in 9610sn2lo (*bottom left*) and 9610sn2hi (*bottom right*) simulations. Every contour represents a 3 m/s increment. The label 9610sn2lo/hi refers to the case of October 1996, and the 2nd simulation with a spectrally nudged formulation with low/high grid resolution

Table 2 Minumum central pressure spread between ensemble members

	lo nn (hPa)	lo sn (hPa)	hi nn (hPa)	hi sn (hPa)
9501 (Jan. 16 at 00 UTC)				
#1	1,010	1,016	1,002	998
#2	1,010	1,016	998	998
#3	1,016	1,018	996	1,004
#4	1,018	1,018	1,000	1,006
0609 (Sept. 26 at 12 UTC)				
#1	996	996	996	996
#2	998	996	996	996
#3	996	996	998	994
#4	998	994	998	996
9609 (Sept. 12 at 06 UTC)				
#1	994	996	992	992
#2	994	996	990	990
#3	994	996	990	990
#4	996	996	992	994
9610 (Oct. 7 at 18 UTC)				
#1	1,006	1,008	1,002	1,002
#2	1,006	1,006	1,002	998
#3	1,006	1,008	1,004	1,002
#4	1,006	1,006	1,006	1,000

The labels #1-#4 indicate the ensemble member; the labels on the first line refer to the different simulations, with the following meaning: "lo nn" refers to low-resolution non-nudged simulations, "lo sn" refers to low-resolution nudged simulations, "hi nn" refers to high-resolution non-nudged simulations, and "hi sn" refers to high-resolution nudged simulations

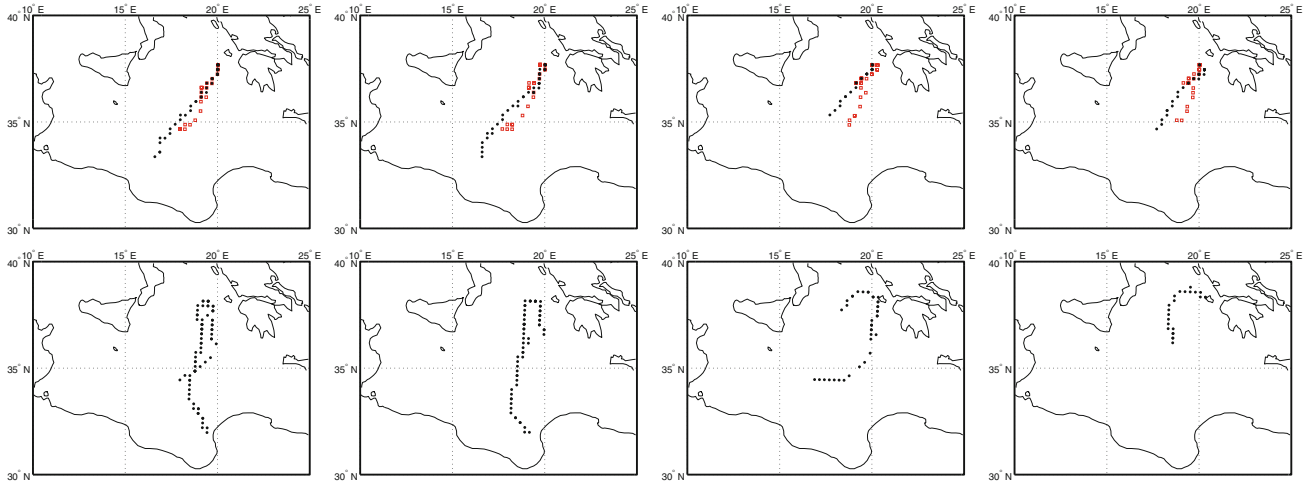

Fig. 14 January 1995 medicane track in the low resolution spectrally nudged 9501sn1lo-9501sn4lo simulations (*top*) and low resolution non nudged 9501nn1hi-9501nn4hi simulations (*bottom*). In the *top panels two different* markers have been used for a better visualiztion: (*red*) empty squares correspond to the part of the track moving northwards, (*blue*) filled circles to the part moving southwards

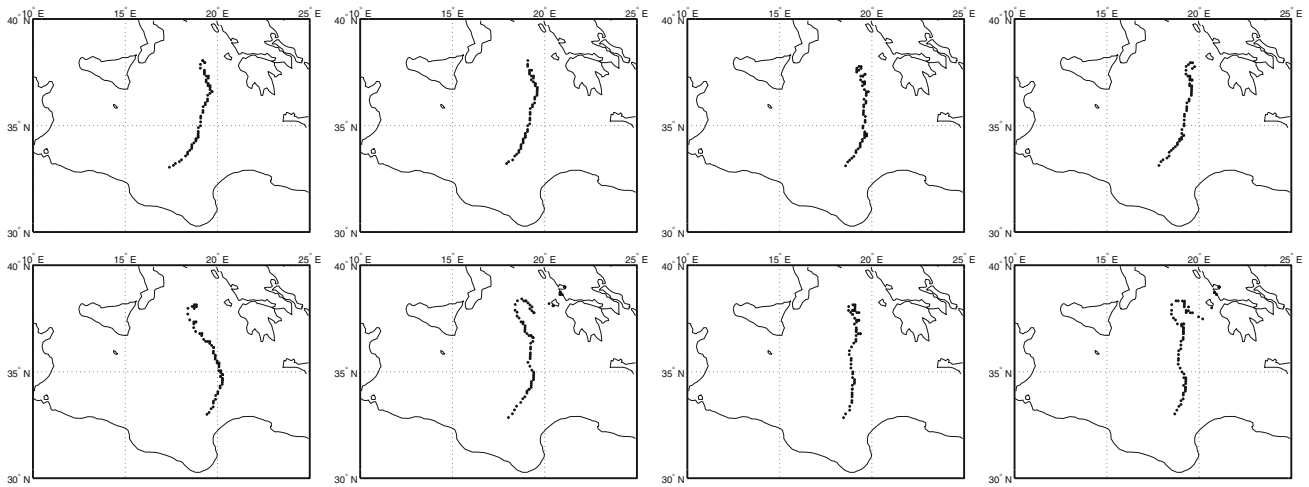

Fig. 15 January 1995 medicane track in the high resolution spectrally nudged 9501sn1lo-9501sn4lo simulations (*top*) and high resolution non nudged 9501nn1hi-9501nn4hi simulations (*bottom*)

of the plot, that is not fully reproduced in the model. Outside of this area however, the presence of the medicane is clearly visible, with simulated winds in the range of 20 m/s. In the NOAA wind field the medicane location corresponds to the cusp in the bottom of the 27 m/s contour.

3.5 The role of spectral nudging

In order to assess the robustness of the results shown above, and the effectiveness of the downscaling procedure applied in the study of medicanes long-term statistics, some evidence is required to support the assumption that the ability of the model to reproduce the medicanes does not depend on the specific initial conditions.

Table 2 shows the spread of minimum central pressure among the different ensemble members, both nudged and non-nudged, for all the four test cases. The largest spread is observed for the 9501 medicane. Figures 14 and 15 show the reconstructed track for the full set of ensemble simulations (with spectral nudging switched on and off, at both 25 km and 10 km resolutions) for the 9501 medicane. As the pictures show, in the low-resolution non-nudged simulations (Fig. 14) the medicane development diverges substantially among the ensemble members. In the nudged simulations on the other hand, the medicane evolution is

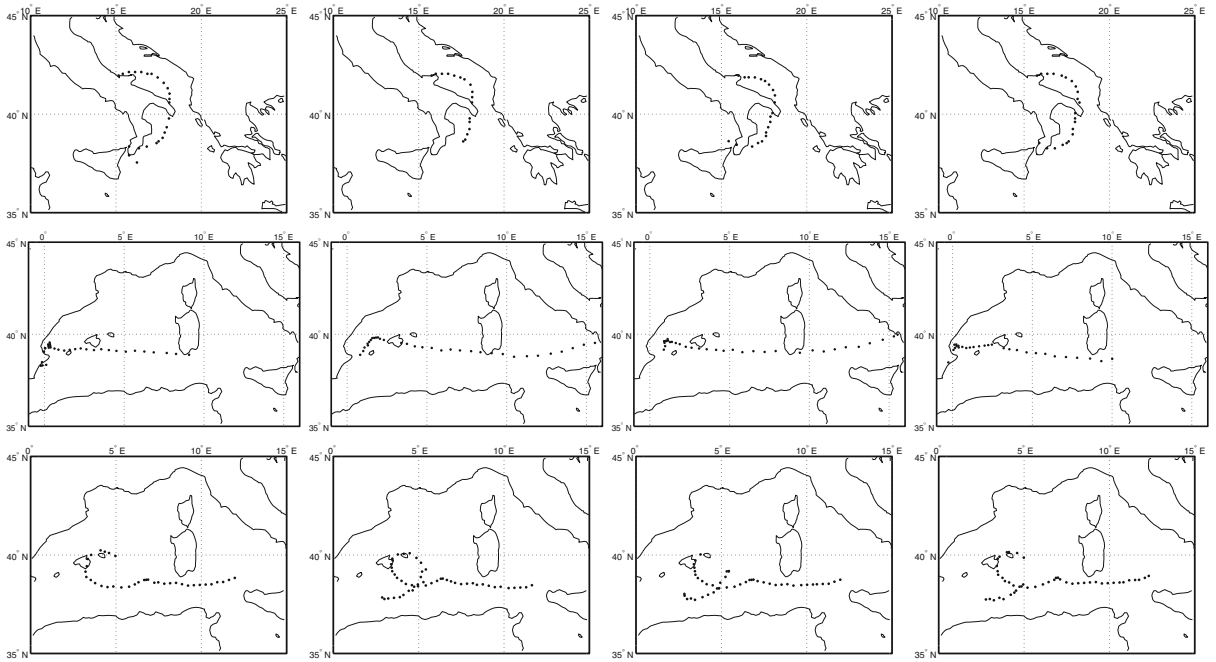

Fig. 16 Medicane track in high resolution spectrally nudged simulations. 0609sn1hi-0609sn4hi simulations for the September 2006 case (*top*), 9609sn1hi-9609sn4hi simulations for the September 1996 case (*middle*) and 9610sn1hi-9610sn4hi simulations for the October 1996 case (*bottom*)

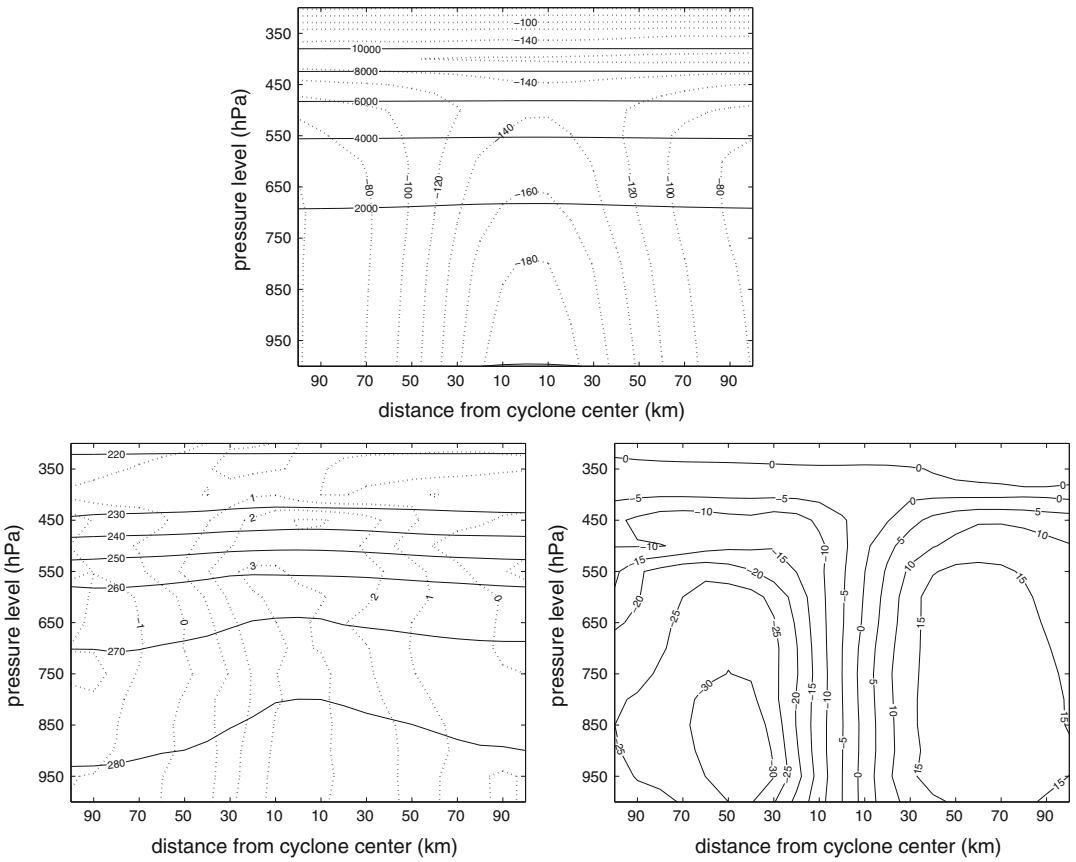

Fig. 17 Vertical profiles of Jan 95 medicane on 01/16 at 00 UTC in spectrally nudged high-resolution 9501sn2hi simulation. *Top*: x–z cross section of geopotential (*full lines*) and geopotential zonal anomaly (*dashed lines*). *Bottom left*: x–z cross section of potential temperature (*full lines*) and potential temperature anomaly (*dashed lines*). *Bottom right*: x–z cross section of y component of velocity

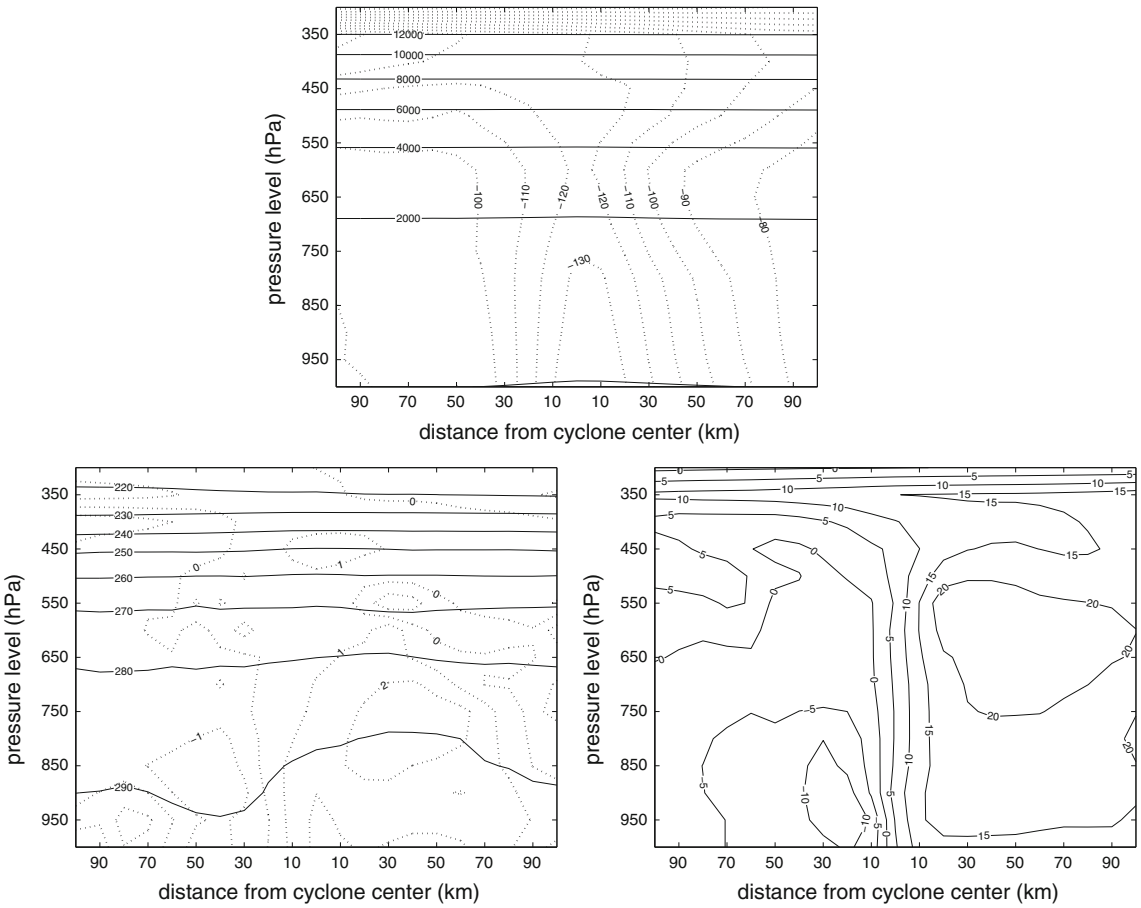

Fig. 18 The same of Fig. 17 for September 06 medicane, on 09/26 at 12 UTC in 0609sn2hi simulation

similar in all the simulations. Even if the evolution of the storm among the high-resolution simulations (Fig. 15) is more similar than in the low-resolution results, the ensemble variability in the spectrally nudged simulations is markedly smaller than in the case without employing the large scale constraint.

In the 0609 case, even if the spread in minimum central pressure among ensemble members reported in Table 2 is limited, in two of the four high-resolution non-nudged simulations (not shown) the simulated storms are weaker in comparison with the corresponding nudged simulation—exhibiting in particular smaller pressure gradients. As a result, the tracking algorithm fails to capture the medicane formation and evolution in those ensemble members. Among the nudged simulations, the storm life cycle is correctly reproduced and tracked in all the ensemble members.

In the two remaining cases, the medicane formation and life cycle is tracked in all the simulations, at both low and high resolution. The inter-ensemble variability is bigger in the non-nudged ensembles.

In order to stress the importance of nudging in enhancing the model ability to reliably reproduce the formation and life cycle of medicanes irrespective of initialisation, we show in Fig. 16 the reconstructed tracks in the nudged high resolution ensemble simulations for the 0609, 9609 and 9610 medicanes.

The results discussed above show how spectral nudging is a crucial feature to ensure that the effect of the nonlinear chaotic regional dynamics generated by the regional model does not drive the system to a different large scale state with respect to the one described by the external fields—so that the synoptic conditions triggering the medicane development may not be present.

4 Results: vertical structure

So far we have devoted our attention to the analysis of the sea level wind and pressure patterns associated with medicanes. However, in order to study the features related to the tropical-like nature of medicanes, such as for example their axis-symmetry or warm core, the full vertical structure of the cyclone has to be taken into account.

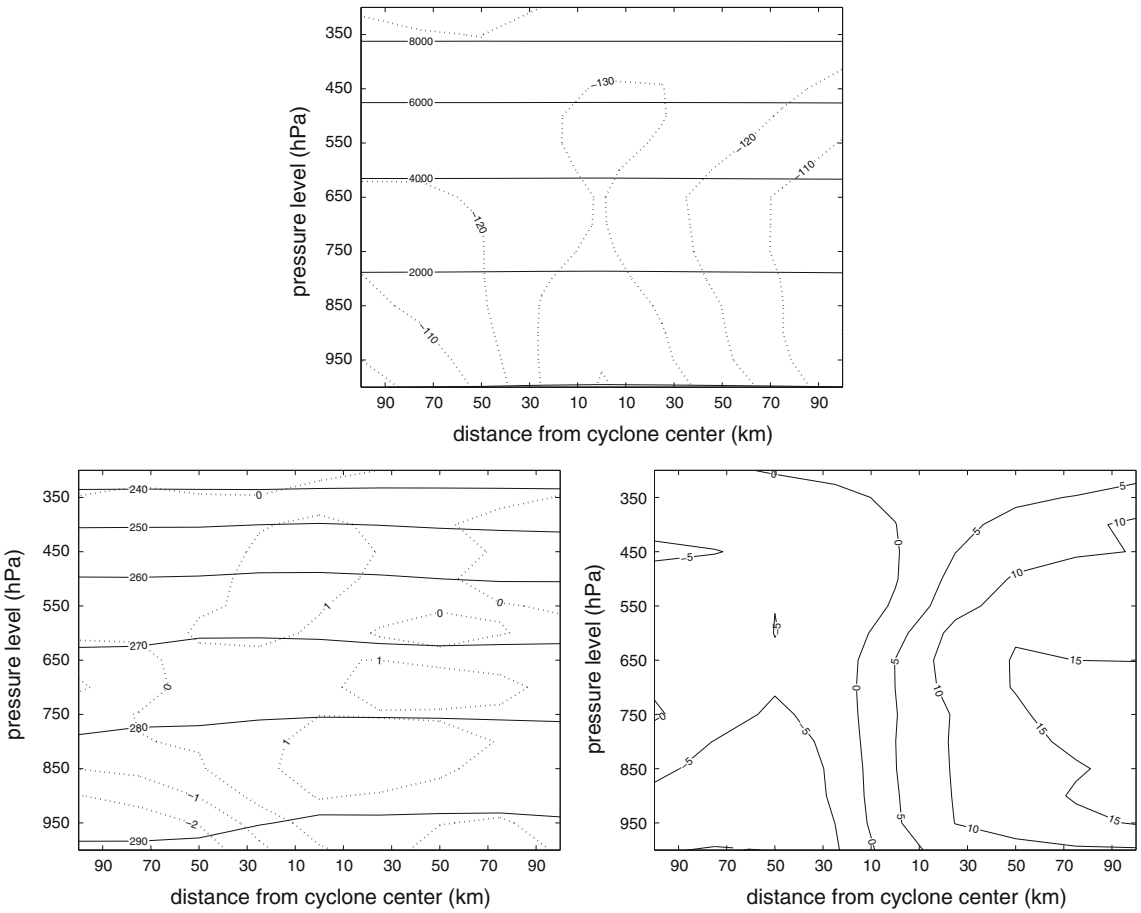

Fig. 19 The same of Fig. 18 in 0609sn2lo low-resolution simulation

Besides giving an insight on the dynamical characterization of medicanes, the analysis of their vertical structure has also a practical interest. Several modelling studies on tropical cyclones (Walsh 1997; Walsh et al. 2007; Hart 2003) in fact exploited features of the TCs 3D structure to detect and track them in the model output. It is thus interesting to investigate whether a similar characterization can be applied to the medicanes.

We will focus on the variables that are expected to reflect the most typical signatures of a tropical-like cyclone dynamics: geopotential, potential temperature and horizontal velocity.

Figures 17 and 18 show distributions of the aforementioned variables for, respectively, the 9501 and 0609 cases, in the spectrally nudged high resolution simulations. The two remaining cases (not shown) exhibit a similar behavior. The geopotential profiles show an almost perfect axis-symmetric structure, extending up to 300 hPa. In all the cases, positive temperature anomalies are found in the vicinity of the cyclone center, reflecting the medicanes warm core structure. Velocity profiles show as well a structure very similar—at a smaller scale—to the one of tropical cyclones, characterized by a region in the center of the storm with very low wind speed, corresponding to the cyclone's eye; outside of this region, wind speed has a maximum a few grid points away from the storm center, in the lower troposphere, and then decreases upwards and outwards. The region of maximum wind is interpreted as being associated with the eyewall.

Figure 19 shows profiles corresponding to Fig. 18 in a coarse resolution run for the 0609 medicane. While the typical structure of the geopotential and velocity profiles is still visible, it is more difficult to keep track of the warm core structure. In the velocity profile, the region of maximum winds is displaced farther from the cyclone center, reflecting a poorer representation of the eye structure. Similar differences between low and high resolution vertical profiles emerge from the analysis of the remaining cases.

5 Conclusions and outlook

In the present study we showed that a high resolution regional climate model (CCLM) driven by boundary conditions derived by NCEP/NCAR renalysis is able to reproduce a number of medicanes test cases, provided

spectral nudging is applied. Not only are the medicanes generated at about the correct time and location, but also their internal dynamical structure, including characteristic features such as vertical symmetry and warm core, is well simulated. For both the surface variables and the vertical structure, most details are fully resolved only in the high resolution simulations.

The degree of accuracy of the values of the atmospheric fields produced by the model in the vicinity of the storm depends on the resolution. The depths of pressure minima coincide with good accuracy with the observed ones in the low resolution simulation, while a deepening due to the better resolved cyclone fine structure is generally observed in the high resolution simulations. The value of wind speed, on the other hand, tends to be underestimated by 10–30% in the coarse resolution simulations.

These results suggest that performing the dynamical downscaling of reanalyses data is an effective method to investigate long-term statistics of the emergence, tracking and of dynamical properties of medicanes.

Acknowledgments We acknowledge Burkardt Rockel and Beate Geyer for their precious help with the model. We thank Silvio Gualdi, Antonio Navarra and Matthias Zahn for many valuable and stimulating discussions.

References

Conte D, Miglietta MM, Levizzani V (2011) Analysis of instability indices during the development of a Mediterranean tropical-like cyclone using MSG-SEVIRI products and the LAPS model. Atmos Res 101:264–279

Davolio S, Miglietta MM, Moscatello A, Pacifico F, Buzzi A, Rotunno R (2009) Numerical forecast and analysis of a tropical-like cyclone in the Ionian Sea. Nat Hazards Earth Syst Sci 9:551–562

Ebuchi N, Graber HC, Caruso MJ (2002) Evaluation of wind vectors observed by QuikSCAT/SeaWinds using ocean buoy data. J Atmos Oceanic Technol 19:2049–2062

Emanuel K (2005) Genesis and maintenance of "Mediterranean hurricanes". Adv Geosci 2:217–220

Feser F, von Storch H (2008) A dynamical downscaling case study for typhoons in SE Asia using a regional climate model. Mon Weather Rev 136:1806–1815

Fita L, Romero R, Luque A, Emanuel K, Ramis C (2007) Analysis of the environments of seven Mediterranean tropical-like storms using an axisymmetric, nonhydrostatic, cloud resolving model. Nat Hazards Earth Syst Sci 7:41–56

Hart RE (2003) A cyclone phase space derived from thermal wind and thermal asymmetry. Mon Weather Rev 131:585–616

Homar V, Romero R, Stensrud DJ, Ramis C, Alonso S (2003) Numerical diagnosis of a small, quasi-tropical cyclone over the western Mediterranean: dynamical vs. boundary factors. Q J R Meteorol Soc 129:1469–1490

Kalnay E et al (1996) The NCEP/NCAR 40-year reanalysis project. Bull Am Meteor Soc 77:437–470

Lagouvardos K, Kotroni V, Nickovic S, Jovic D, Kallos G, Tremback CJ (1999) Observations and model simulations of a winter sub-synoptic vortex over the central Mediterranean. Meteorol Appl 6:371–383

Luque A, Fita L, Romero R, Alonso S (2007) Tropical-like Mediterranean storms: an analysis from satellite. In: EUMETSAT 07 proceedings. http://www.eumetsat.int/Home/Main/AboutEUMETSAT/Publications/ConferenceandWorkshopProceedings/2007/SP_1232700283028?l=en

Miglietta MM, Moscatello A, Conte D, Mannarini G, Lacorata G, Rotunno R (2011) Numerical analysis of a Mediterranean "hurricane" over south-eastern Italy: Sensitivity experiments to sea surface temperature. Atmos Res 101:412–426

Moscatello A, Miglietta MM, Rotunno R (2008) Numerical analysis of a Mediterranean "hurricane" over south-eastern Italy. Mon Weather Rev 136:4373–4396

Moscatello A, Miglietta MM, Rotunno R (2008) Observational analysis of a Mediterranean "hurricane" over south-eastern Italy. Wheather 63:306–311

Pytharoulis I, Craig G, Ballard S (2000) The hurricane-like Mediterranean cyclone of January 1995. Meteorol Appl 7:261–279

Rasmussen E, Turner J (2003) Polar lows: mesoscale weather systems in the polar regions. Cambridge University Press, Cambridge

Reale O, Atlas R (2001) Tropical cyclone-like vortices in the extratropics: observational evidence and synoptic analysis. Weath For 16:7–34

Ricciardulli L, Wentz F (2011) Reprocessed QuikSCAT (V04) wind vectors with Ku-2011 geophysical model function. Technical Report 043011, Remote Sensing Systems

Rienecker MM et al (2011) MERRA: NASA's modern-era retrospective analysis for research and applications. J Clim 24:3624–3648

Rockel B, Will A, Hense A (2008) The regional climate model COSMO-CLM (CCLM). Meteorol Z 17:347–348

Simmons AJ (2006) Observations, assimilation and the improvement of global weather prediction—some results from operational forecasting and ERA-40. In: Palmer T, Hagedorn R (eds) Predictability of weather and climate. Cambridge University Press, Cambridge

Tous M, Romero R (2011) Medicanes: creació d'una base de dades i exploració dels ambients meteorològics. Tethys 8, to appear

von Storch H, Langenberg H, Feser F (2000) A spectral nudging technique for dynamical downscaling purposes. Mon Weather Rev 128:3664–3673

Walsh K (1997) Objective detection of tropical cyclones in high-resolution analyses. Mon Weather Rev 125:1767–1779

Walsh KJE, Fiorino M, Landsea CW, McInnes KL (2007) Objectively determined resolution-dependent threshold criteria for the detection of tropical cyclones in climate models and reanalyses. J Clim 20:2307–2314

Zahn M, von Storch H (2008) Tracking polar lows in CLM. Meteorol Z 17:445–453

Zahn M, von Storch H, Bakan S (2008) Climate mode simulation of North Atlantic polar lows in a limited area model. Tellus 60A:620–631

Zhang HM, Bates JJ, Reynolds RW (2006) Assessment of composite global sampling: Sea surface wind speed. Geophys Res Lett 33:L17,714